CHEMISTRY
A European Journal

A Journal of
ChemPubSoc Europe

Accepted Article

Title: Rh complexes of a new generation sapphyrin: unique structures, axial chirality, and catalysis thereby

Authors: Zeev Gross, Qiu-Cheng Chen, Irena Saltsman, Natalia Fridman, Zi-ye Xiao, Xuan Zhan, and Alexander Kaushansky

To be cited as: *Chem. Eur. J.* 10.1002/chem.201804138

Link to VoR: http://dx.doi.org/10.1002/chem.201804138

Supported by
ACES

WILEY-VCH

10.1002/chem.201804138

WILEY-VCH

Rh complexes of a new generation sapphyrin: unique structures, axial chirality, and catalysis thereby

Qiu-Cheng Chen, Irena Saltsman, Alexander Kaushansky, Zi-ye Xiao, Natalia Fridman, Xuan Zhan, and Zeev Gross*

Abstract: Rhodium insertion into the new 5,10,15,20-tetra(trifluoromethyl)sapphyrin was found to be much more facile than for other analogues, attributable to unique NH-F hydrogen bonding interactions that stabilize the pyrrole-inverted structure characteristic of the metallated product. The thus obtained rhodium(I) complexes are of axial chirality and the enantiomers were resolved. The latter were found to interconvert quite fast in a process that involves a tautomerization-like movement of the metal fragment between the five N atoms. Also reported is the examination of the rhodium sapphyrins as catalysts for organic synthesis, performed by looking into their carbene-transfer activity using cyclopropanation of styrene by ethyl diazoacetate (EDA) and comparing it to rhodium corroles.

Introduction

Metal complexes of porphyrins and related macrocycles play indispensable roles in numerous catalytic biochemical processes,[1] which continues to be the motivation for research on expanded, contracted and modified porphyrins.[2] The first isolated free-base porphyrin appears to be hematoporphyrin (named cruentine by Thudichum who reported it in 1867),[3] while the first expanded and contracted porphyrin analogs were reported around 100 years later: sapphyrins by Woodward[4] and corroles by Johnson.[5] Common to all three macrocycles is an aromatic conjugation pathway and fast tautomerism that makes all inner N atoms equivalent.[6] The features shared by sapphyrins and corroles are: the principle rotation axis being C_2 rather than C_4 in porphyrins; the presence of two directly linked pyrrole rings; and three NHs rather than two in porphyrins (Scheme 1). The last mentioned property remains the main driving force for the extensive investigation of the very rich and often unique coordination chemistry of metal ions chelated by corroles.[7] Metalation of corroles by transition/post-transition metal ions is not only facile, but in fact often stabilizes the ligand and induces diverse functions.[8] These factors and the revolutionary improvements of free-base corrole synthesis (such as **H_3(tpfc)**, 5,10,15-tris-(pentafluorophenyl)-corrole) during the last two decades led to the introduction of metallocorroles as catalysts for organic, inorganic, and bioinorganic processes relevant to the worldwide efforts devoted to cleaner energy resources and disease fighting.[9]

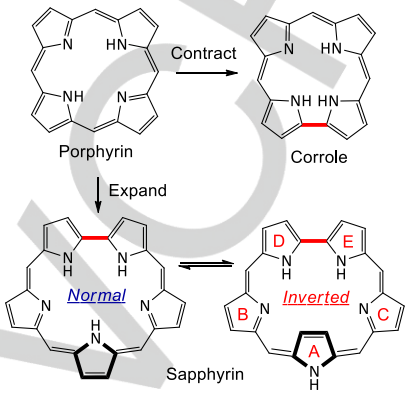

Scheme 1. The basic structures of porphyrin, corrole and sapphyrin, with the bipyrrole moieties of corrole and sapphyrin highlighted in red and the latter drawn in the normal and inverted conformations that are common for the β-pyrrole and *meso*-C-substituted sapphyrins, respectively. One particular tautomer is drawn in all cases.

Sapphyrin chemistry is by large focused on the free-base derivatives with impressive achievements in their utilization as anion and cation receptors, PDT sensitizers and nonlinear optical materials.[10] Meanwhile, their coordination chemistry remained limited,[10b,11] and only rhodium complexes were reported for *meso*-aryl-substituted sapphyrins.[11,12] The two reasons for the restricted progress are: a) the N5 core of sapphyrins is a much less suitable coordination sphere than the-

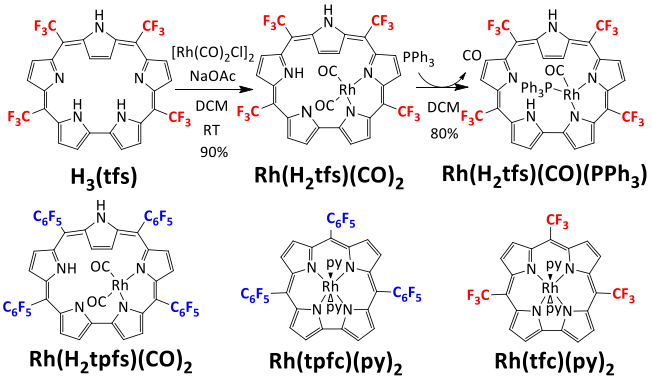

Scheme 2. Synthesis of **$Rh(H_2tfs)(CO)_2$** and **$Rh(H_2tfs)(CO)(PPh_3)$** and drawing of the rhodium complexes of the other expanded or contracted porphyrin mentioned in the text (py = pyridine). Note that the location of the inner NH protons in the free-base sapphyrin is tentative only.

-N4 core present in porphyrins and corroles and b) pyrrole ring A rotation (Scheme 1) dramatically alters the chelating properties of the sapphyrin core.[10a,13] Neutral *meso*-aryl-substituted sapphyrins have only recently been fully characterized,

[*] Prof. Z. Gross, Dr. I. Saltsman, Dr. Alexander Kaushansky, Dr. N. Fridman, Q. C. Chen, Z. Y. Xiao, and X. Zhan
Schulich Faculty of Chemistry
Technion-Israel Institution of Technology
Haifa 32000 (Israel)
E-mail: chr10zg@technion.ac.il

Supporting information and the ORCID identification number(s) for the author(s) of this article can be found under:

disclosing structures both with and without an inverted pyrrole ring A.[14,11] Truly surprising is that there is just a single case that metal complexes of sapphyrins were claimed to be useful for catalysis, which was one motivation for the current research.[15] The other one was that we recently gained access to the first *meso*-alkyl-substituted sapphyrin,[16] which displayed several novel features, and it was hence of interest to see if and how they may come into effect in practical applications. We now report the results obtained with five rhodium complexes, chelated by sapphyrins and corroles with either C_6F_5 or CF_3 groups on their respective *meso*-C atoms (Scheme 2).

Results and Discussion

Insertion of rhodium into the new 5,10,15,20-tetra(trifluoromethyl)sapphyrin, **H_3(tfs)**, appeared to be much more facile (1 h, RT, 90% yield) than for 5,10,15,20-tetra(pentafluorophenyl)-sapphyrin **H_3(tpfs)**,[12] which is reminiscent of the mild reaction condition for metallation of heterosapphyrin.[17] The decrease in symmetry from C_{2v} to C_1 upon metalation came into effect by four instead of two CF_3-attributed signals in the ^{19}F NMR spectrum (Figure S1), as well as in the doubling of the number of ^1H NMR resonances due to the normal and inverted β-pyrrole-H atoms (Figure 1a).[10b] The molecular structure of the product was deduced to be **Rh(H_2tfs)(CO)$_2$**, composed of a d^8 low-spin rhodium(I) metal center coordinated by two N atoms of the mono-anionic macrocycle and two carbonyls. This is consistent with its high-resolution mass spectrum (Figure S10), the sharp ^1H NMR spectrum and the appearance of two NH protons therein (Figure 1a). The about 15 ppm difference in the chemical shift of these two protons clearly indicates that pyrrole ring A (Scheme 1) remains inverted after metalation (and even when treated with up to 40 equivalents of trifluoroacetic acid). This is reminiscent of the previously reported *meso*-C_6F_5 analogue **Rh(H_2tpfs)(CO)$_2$**,[12] but different from the Rh(I) and Ir(I) complexes of β-pyrrole-alkylated sapphyrins wherein all pyrroles are not inverted[15] and also from the Rh(I) complexes of *meso*-aryl heterosapphyrin wherein the metal ion is coordinated by the N atoms of the bipyrrole sub-unit.[17a]
Confirmation of the above conclusions was obtained by the X-ray crystal structures of both **Rh(H_2tfs)(CO)$_2$** (Figure 1b-d) and **Rh(H_2tpfs)(CO)$_2$** (Figure 2), which also disclosed the following information. The dihedral angles of the most deviating pyrrole ring A were found to be roughly 35° (Figures 1d and S17b) and the mean plane deviations (MPD) of **Rh(H_2tfs)(CO)$_2$** and **Rh(H_2tpfs)(CO)$_2$** are 0.268 Å and 0.176 Å respectively. The latter values are surprisingly close to those reported for the Rh(I) complex of a sapphyrin that does not have an inverted pyrrole ring[11], due to the presence of both *meso*-C_6F_5 and β-pyrrole-alkyl substituents. DMF appeared to be necessary for obtaining high quality X-ray crystals of **Rh(H_2tpfs)(CO)$_2$**, likely attributable to fixation of the most flexible pyrrole ring A due to *intermolecular* $_{DMF}O$---$HN_{pyrrole}$ hydrogen bonding interactions (Figure 2). The structure of **Rh(H_2tfs)(CO)$_2$** uncovers *intramolecular* N-H—F bonding interactions (Figure 1b), which provides a hint for much more facile Rh insertion into **H_3(tfs)** relative to **H_3(tpfs)**. In the former but not latter case, the conformation with inverted pyrrole is absolutely preferred even before metallation and there is hence no extra penalty in moving from free-base to the metal complex. We note that the same kind of explanation likely holds for the case where both the free-base sapphyrin and the metal complex do not prefer an inverted pyrrole: for the sapphyrin that has both *meso*-C_6F_5 and β-pyrrole-alkyl substitutents, even the insertion of two rhodium ions has been reported to proceed very smoothly.[11]

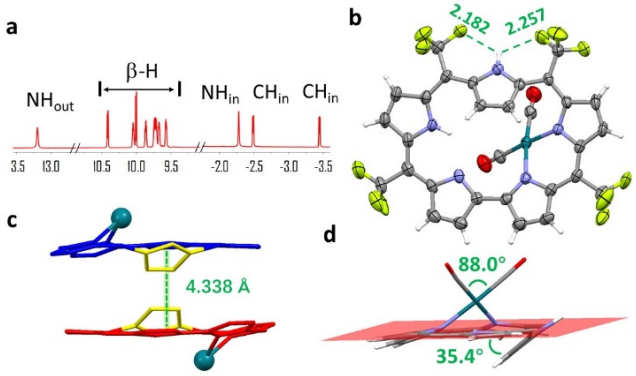

Figure 1. The ^1H NMR spectrum of **Rh(H_2tfs)(CO)$_2$** with assignment of the NH and CH protons of pyrrole ring A (a) and three different views of it molecular structure: (b) front view, with thermal ellipsoids of 50% and highlight of F-HN distances; (c) side view *(meso*-CF_3 and Rh-carbonyl substituents omitted), with emphasis on pyrrole ring A (yellow colored), enantiomers arrangement and the distance between them; (d) side view with emphasis on the square planar coordination sphere of the rhodium(I) center.

Consistent (although often ignored) with the C_1 symmetry, the crystal structures of **Rh(H_2tfs)(CO)$_2$** and **Rh(H_2tpfs)(CO)$_2$** disclose the presence of two enantiomers in a 1:1 ratio (Figure 1c). Separation of the racemic mixture by HPLC with a chiral column was not only quite difficult, but appeared to be non-practical for obtaining pure enantiomers. Injection of the separated fractions revealed the re-formation of a mixture (Figure S20), clearly indicative of a very facile racemization pathway for these complexes.

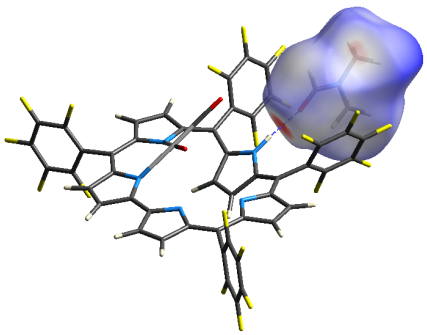

Figure 2. Hydrogen bonding between **Rh(H_2tpfs)(CO)$_2$** and DMF shown by a d_{norm} Hirshfeld surface.

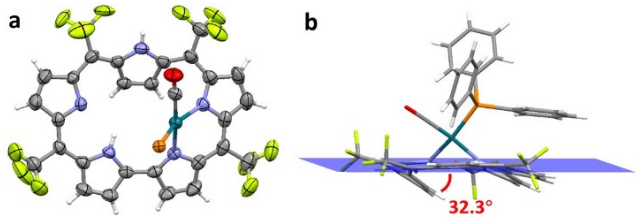

Figure 3. The X-ray crystal structure of **Rh(H$_2$tfs)(CO)(PPh$_3$)**: (a) front view, with thermal ellipsoids of 50% (phenyl groups omitted); (b) side view with emphasis on dihedral angles between pyrrole ring A and the least-square plane.

Considering that one plausible possibility is that the Rh(CO)$_2$ moiety is able to flip through the core, **Rh(H$_2$tfs)(CO)$_2$** was treated with triphenylphosphine (PPh$_3$) for increasing the steric hindrance and blocking that racemization route. ^{1}H NMR analysis of the reaction product, isolated in quite high yield (Scheme 2), easily revealed that only one carbonyl was replaced by **PPh$_3$** (Figure S7) and that pyrrole ring A remained inverted in **Rh(H$_2$tfs)(CO)(PPh$_3$)**. The other analytical data such as high resolution MS (Figure S14) and IR (one rather than two kinds of carbonyl stretches) were also consistent with the **Rh(H$_2$tfs)(CO)(PPh$_3$)** structure, while the position of PPh$_3$ therein was clarified by X-ray crystallography (Figure 3a) to be in the less sterically crowded part of the macrocycle's core. Indeed, attempted replacement of both carbonyls by using either excess of PPh$_3$ or the bidentate ethylenebis(diphenylphosphine) (DIPHOS) induced decomposition rather than formation of any desired product.

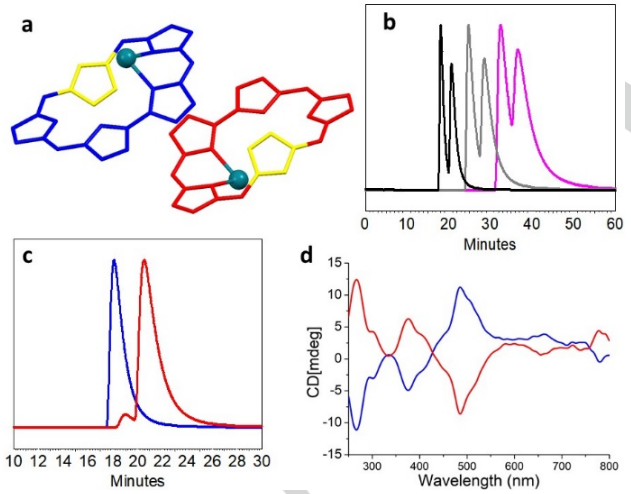

Figure 4. The arrangement of two enantiomers in the X-ray structure of **Rh(H$_2$tfs)(CO)(PPh$_3$)** (*meso*-CF$_3$, carbonyl and PPh$_3$ groups omitted), with emphasis on pyrrole ring A (yellow colored) (a); HPLC profiles (n-hexane as eluent, OD-H column, UV-detector 488 nm, 0.9 mL/min flow rate) of the racemic mixture at 9° (purple trace), 25° (grey trace) and 40° C (black trace) (b); and of the separated fractions at 40° C (c); circular dichroism spectra of the first (blue trace) and the second (red trace) fractions, at room temperature in n-hexane (d).

Similar to **Rh(H$_2$tfs)(CO)$_2$**, the X-ray crystal structure of **Rh(H$_2$tfs)(CO)(PPh$_3$)** disclosed pairs of associated enantiomers with MPD values of 0.263 Å and pyrrole ring A angles of 32.3° (Figure 4a & Figure 3b). In this case, an almost perfect separation of the racemic mixture was achieved by chiral HPLC (Figure 4b-c) and the circular dichroism (CD) spectra of the two enantiomers displayed strong signals in both the UV and the visible parts (Figure 4d). The enantiomers were however still found to be stable only when hexane was used as both eluent and solvent, while fast racemization took place when dichloromethane was used as solvent, reminiscent to what happened with **Rh(H$_2$tfs)(CO)$_2$** (Figure S20). This might suggest that the process responsible for racemization involves movement of pyrrole ring A, as the intramolecular CF$_3$···H-N interactions (Figure 1b) that fix its position and prevent the flip through the core movement of the metal with its ligands are weakened by a polar solvent.

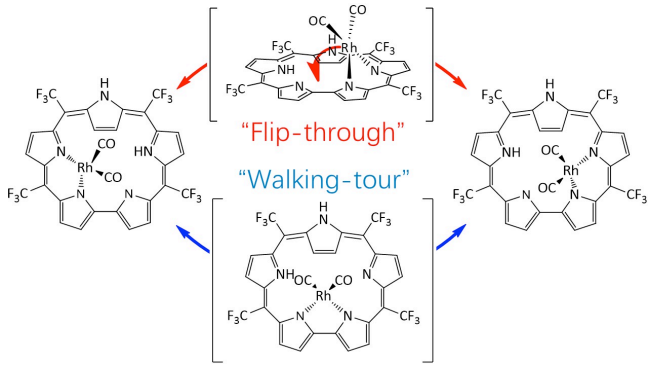

Figure 5. Two proposed racemization mechanism of **Rh(H$_2$tfs)(CO)$_2$**: "Flip-through" (red labeled) and "Walking-tour" (blue labeled) pathways.

The somewhat less facile racemization of **Rh(H$_2$tfs)(CO)(PPh$_3$)** relative to **Rh(H$_2$tfs)(CO)$_2$** (Figure S21) triggered our interest in understanding the racemization pathway. The initial sought was that the Rh(CO)$_2$ sub-unit is able to move through the coordination core (Figure 5, "flip-through") and that this is less facile for the more bulky Rh(CO)(PPh$_3$) moiety present in **Rh(H$_2$tfs)(CO)(PPh$_3$)**. This "flip-through" hypothesis was immediately ruled out by DFT calculations, which confirmed that the strong repulsive interactions between two CO ligands and sapphyrin skeleton prevent the racemization via this mechanism. Potential energy surfaces of alternative "flip-through" pathways, such as of less bulky Rh(CO) and Rh moieties formed in concert with temporary dissociation of CO ligand(s), also passed through intermediates and transition states that are much too high in energy (Figure S25). The same holds for a variety of other investigated mechanisms (Figures S19-21), except of the one that involves migration of both the Rh(CO)$_2$ moiety and protons among the inner core's N atoms (Figures 5-7).

10.1002/chem.201804138

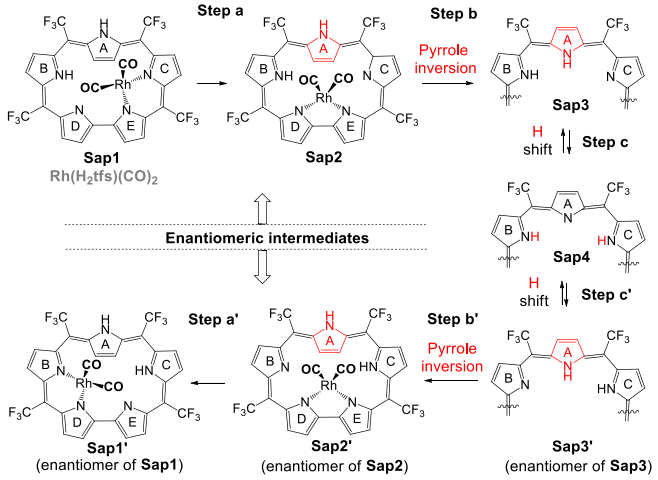

Figure 6. Steps of "walking" pathway basing on DFT study. The movement of pyrrole ring A and the NH proton(s) were highlighted in red.

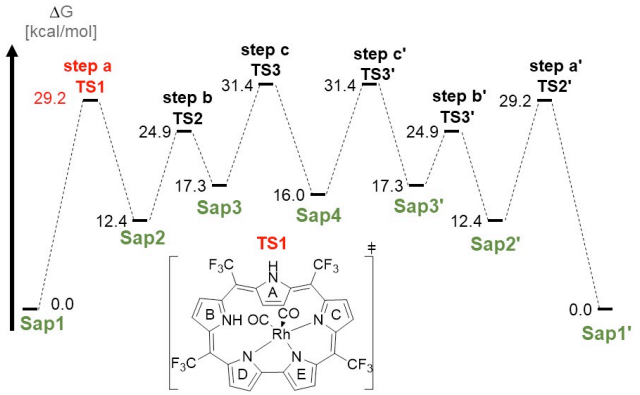

Figure 7. Free-energy profile for racemization mechanism in DCM at PBE0-D3(BJ)/BS2//PBE0-D3(BJ)/BS1 level of theory and the proposed structure of TS1.

One key feature of the "walking tour" pathway is the 29.2 kcal/mol barrier transformation of **Sap1** to **Sap2** (step a in Figures 6 and 7), which is substitution of N_C by N_D via the 5-coordinate transition state **TS1** (N_A, N_B, N_C, N_D, and N_E are the N atoms of the respective pyrrole rings). Further walking of the $Rh(CO)_2$ moiety would produce **Sap1'**, the enantiomer of **Sap1**, but that does not happen because of a formidably high energy barrier for direct proton transfer between N_B and N_C. Inversion of pyrrole A as to produce **Sap3** does however proceed through a relatively low-lying transition state (step b) and that may now be followed by much more facile proton transfer from N_A to N_C (step c). The thus formed non-chiral intermediate **Sap4** may return to either **Sap1** or **Sap1'** by reversal of the described steps, thus completing the racemization process. Transition state **TS3** is of the highest energy (31.8 kcal/mol) in that mechanism and it includes the inversion of ring A. This might be the rational for the slower racemization rate in hexane, wherein the loss of $CF_3\cdots$H-N interactions upon moving from **Sap3** to **Sap4** could be most significant.

Armed with the acquired knowledge on the Rh(I) complexes of the two sapphyrins, their potential catalytic activity was addressed, in comparison with the rhodium(III) complexes of corroles with the same *meso*-C substitutents. **$Rh(tpfc)(py)_2$** was already reported as good catalysts for carbene-transfer reactions;[18] and we have now prepared the much smaller **$Rh(tfc)(py)_2$**. The ^{19}F and ^{1}H NMR spectra (Figure S4) allowed for full characterization of this new corrole, including the identification of two pyridine molecules that are strongly bound to the metal. These conclusions were fully confirmed by analysis of the X-ray structure (Figure 8a), which disclosed Rh-$N_{pyridine}$ bond lengths of 2.065(5) Å, in the range of other Rh(III) corroles.[18] With a MPD of 0.05, **$Rh(tfc)(py)_2$** may be considered as practically planar, in contrast with its sapphyrin analogs **$Rh(H_2tfs)(CO)_2$** and **$Rh(H_2tfs)(CO)(PPh_3)$** that have a flexible pyrrolic unit and a rhodium(I) centre of square planar geometry-

-using only two N atoms for coordination to the metal centre (Figure 8b). The effect of CF_3 *vs.* C_6F_5 on the redox potential for the sapphyrin was larger than for corroles, with positive shifts of 340 and 190 mV, respectively (Figure 9). Also noteworthy is that the redox processes of the corroles were much more reversible than those of the sapphyrins, a phenomenon that will be addressed only in future studies as it requires multiple approaches for studying these potentially non-innocent ligands.[19]

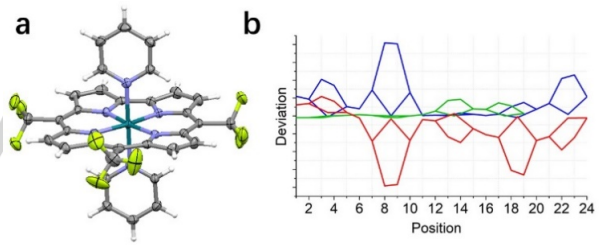

Figure 8. (a) Crystal structure of **$Rh(tfc)(py)_2$**; (b) Mean-plane deviation diagram calculated from the core atoms for **$Rh(tfc)(py)_2$** (green), **$Rh(H_2tfs)(CO)_2$** (blue) and **$Rh(H_2tfs)(CO)(PPh_3)$** (red).

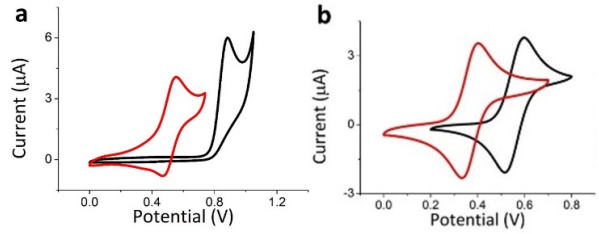

Figure 9. Cyclic voltammetry (RT, CH_2Cl_2, 0.5 mM substrate, 0.1 M TBAP, glassy carbon working electrode, 50 mVs^{-1} scan rate, vs. $Fc^{+/0}$ in 25 mV) of (a) **$Rh(H_2tfs)(CO)_2$** (black trace) and **$Rh(H_2tpfs)(CO)_2$** (red trace); and (b) **$Rh(tfc)(py)_2$** (black trace) and **Rh(tpfc)(py)2** (red trace). The corresponding square wave spectra of the sapphyrin rhodium complexes are provided in Figure S22.

All examined complexes were found to be good catalysts for the model reaction:[20] cyclopropanation of styrene by ethyl diazoacetate (EDA**,** Scheme 3 and Table 1). The complexes with *meso*-C_6F_5 groups, **Rh(tpfc)(py)$_2$** and **Rh(H$_2$tpfs)(CO)$_2$**, were more selective regarding cyclopropanation vs. EDA dimerization and *anti* vs. *syn* products, than **Rh(tfc)(py)$_2$** and **Rh(H$_2$tfs)(CO)$_2$** with their *meso*-CF_3 substituents. Considering that the rate limiting step in these reaction is commonly the formation of the metal-carbene intermediate and not the pre-association of EDA to the metal complex,[21] the above deduced stronger electron withdrawing effect of CF_3 relative to C_6F_5 is apparently disadvantageous for this kind of reaction. Meanwhile, the significant yields of the less stable *syn*-isomer are reminiscent of other corrole and porphyrin-base catalysts (Entry 1, 2, 5&6).[18, 22] An attempt of further increasing the relative amounts of that isomer by increasing the steric hindrance around the metal center by CO/PPh_3 substitution was successful (the last two entries of Table 1), but that came with a price. The total yield was much lower, probably due to the earlier noticed diminished stability of the catalysts.

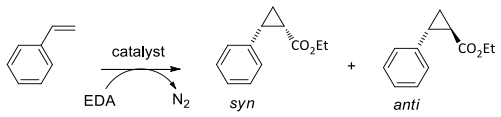

Scheme 3. Metallosapphyrin/metallocorrole-catalyzed cyclopropanation of styrene by ethyl diazoacetate (EDA).

Table 1. Cyclopropanation of styrene by ethyl diazoacetate (EDA) catalysed by the rhodium(I) and rhodium(III) complexes depicted in Scheme 2.[a]

Catalyst	Yield of diethyl maleate	Yield of cyclopropyl esters	anti/syn ratio
Rh(tpfc)(py)$_2$	2%	85%	2.3
Rh(tfc)(py)$_2$	2%	36%	2.0
Rh(H$_2$tpfs)(CO)$_2$	3%	82%	3.0
Rh(H$_2$tfs)(CO)$_2$	3%	68%	2.3
Rh(H$_2$tpfs)(CO)(PPh$_3$)[b]	1%	16%	1.8
Rh(H$_2$tfs)(CO)(PPh$_3$)	1%	19%	1.7

[a] catalyst/EDA/styrene = 1/500/5000, addition of EDA in one portion, 0.28-0.30 mM of catalyst, under Ar, in dichloromethane, at room temperature for 24 h. Yields were determined by GC, relative to an internal standard. [b] This complex was not isolated, but prepared *in situ* via addition of 1.6 eq. of PPh_3, based on a titration experiment monitored by UV-vis spectroscopy (Figure S16).

Conclusions

Four novel rhodium complexes, three chelated by monoanioinic sapphyrin and one by trianionic corrole, were synthesized and fully characterized in this study. The emphasis was on deducing their structural and electronic properties, including elements of chirality, as the prerequisite for the application of metallosapphyrins, which is a surprisingly unfertilized field. We trust that the level of understanding provided in this study will lead to the introduction of these very interesting aromatic[23] but yet quite flexible molecules[24] as metal-supporting ligands in many applications much beyond the one we have introduced here.

Experimental Section

Computational details

All DFT calculations reported in this work were carried out using the G09 quantum chemical software.[25] Single-point energy calculations were carried out at the PBE0-D3(BJ)/BS2//PBE0-D3(BJ)/BS1[26] level of theory with solvation effects modeled by IEFPC[27] in dichloromethane, BS1 denoting a mixed basis set of the quasi-relativistic Stuttgart–Dresden–Cologne (SDD) effective core potential and basis set (SDD) for Rh[28], and 6-31+g for all other atoms. While BS2 denoting a mixed basis set of effective core-potential and basis SDD for Rh, and def2-tzvp for all other atoms. Transition-state structures were confirmed to connect corresponding reactants and products by intrinsic reaction coordinate (IRC) calculations.[29]

Instrumentations

All routine chemical reagents and solvents were purchased from commercial sources and were purified by standard procedures before use. Column chromatography was performed on silica gel (Kieselgel 60, 230-400 mesh). ^{1}H and ^{19}F NMR spectra were recorded on Bruker Avance III 400 spectrometer (400 MHz for ^{1}H and 377 MHz for ^{19}F). Chemical shifts are reported in ppm relative to the residual hydrogen atoms in the deuterated solvent $CDCl_3$ (δ = 7.26). High-resolution mass spectra for the compounds were performed on a Bruker MaXis Impact mass spectrometer. Absorption spectra of the samples were measured on HP 8453 diode array spectrometer. Electrochemical measurements were recorded with an EmStat3+ electrochemical system. All the potentials are referenced versus the $Fc^{+/0}$ redox potential added as an internal standard ($E_{1/2}$ = 0.025 V vs. Ag/Ag^+ in 0.1 M TBAP / 0.01 M $AgNO_3$ solution). A conventional three electrode system consisting of a glassy carbon working electrode, a platinum wire as counter electrode and silver wire separated from the bulk solution by a sample holder with a porous glass frit in 0.1 M TBAP / 0.01 M $AgNO_3$ solution. HPLC analysis are performed on a combination of Elite LaChrom organizer, diode array detector L-2455, auto-sampler L-2200, oven L-2300 and pump L-2130. Flow rate: 0.3-1 ml/min; eluent: 100% n-hexane; column: CHIRALCEL® OD-H, 250 x 4.6mm ID. A GC system consist of Sion 4210 GC System and Astec® CHIRALDEX® B-PM Capillary GC Column (L × I.D. 30 m × 0.25 mm, d_f 0.12 µm) was used for calculating the *syn*/*trans* ration as well as the relative amount of dimerization product. Hirshfeld surface calculations[30] were performed by using the program CrystalExplorer 3.1[31]. Hirshfeld surfaces with d_{norm} were mapped on **Rh(H$_2$tpfs)(CO)$_2$**. d_{norm} is a *normalised contact distance*.

X-Ray Crystallographic Details

Single crystals immersed in Paratone-N oil were quickly fished with a glass rod and mounted on a Kappa CCD diffractometer under a cold stream of nitrogen at 200 K. Data collection was

carried out with monochromated Mo Kα radiation using φ and ω scans to cover the Ewald sphere.[32] Accurate cell parameters were obtained with complete collections of intensities, and these were corrected in the usual way.[33] The structure was solved by SHELXS-97 direct methods[34] and refined by the SHELXL-97 program package. The atoms were refined anisotropically. Hydrogen atoms were calculated using the riding model.

Synthesis of H_3(tfs), H_3(tpfs), Rh(tpfc)(py)$_2$, and Rh(H_2tpfs)(CO)$_2$.

The synthetic details for the preparation of **H_3(tfs)**, **H_3(tpfs)**, **Rh(tpfc)(py)$_2$**, and **Rh(H_2tpfs)(CO)$_2$** were provided in pervious publication.[12, 16, 18, 35]

Synthesis of 5,10,15,20-tetra(trifluoromethyl)sapphyrinato dicarbonylrhodium(I) (Rh(H_2tfs)(CO)$_2$).

H_3(tfs) (50 mg) was dissolved in dichloromethane (50 mL). Excess amount of anhydrous sodium acetate was added to the solution followed by di-μ-chloro-bis[dicarbonylrhodium(I)] (20 mg), and the mixture was stirred for 1 hour monitored by TLC (DCM/n-hexane = 1/9) to show a fully conversion. The solvent was evaporated in vacuo, and the residue was chromatographed a silica column (DCM/n-hexane = 1/99). The golden brown fraction was collected (55 mg, 90 % yield), and recrystallized in DCM/hexanes to give green crystals. ^{1}H NMR (400 MHz, $CDCl_3$) δ = 13.20 (s, 1H), 10.42 (d, *J* = 4.5, 1H), 10.05 (d, *J* = 2.3, 1H), 10.01 (d, *J* = 4.9, 1H), 9.87 (dd, *J* = 4.9, 2.5, 1H), 9.78-9.71 (app. ddd, *J* = 10.5, 4.9, 2.5, 2H), 9.68 (d, *J* = 2.4, 1H), 9.58 (dd, *J* = 4.7, 2.0, 1H), -2.28 (s, 1H), -2.47 (dd, *J* = 4.8, 1.6, 1H), -3.42 (dd, *J* = 4.8, 1.6, 1H). ^{19}F NMR (377 MHz, $CDCl_3$) δ = -36.62 (s, 3H), -39.00 (s, 3H), -46.34 (s, 3H), -48.61 (s, 3H).HRMS$^-$ (ACPI, negative mode) for $C_{30}H_{12}F_{12}N_5O_2Rh$: m/z = 804.9854 (calculated), 804.9860 (observed). UV-vis (toluene): max (ε(M^{-1} cm^{-1})) = 357 nm (23500), 491 (116000), 642 (10600), 697 (12200), 764 (5400), 876 (6200). IR (neat, cm^{-1}): 2067, 2002.

Synthesis of 5,10,15,20-tetra(trifluoromethyl)sapphyrinato triphenylphosphine-carbonylrhodium(I) (Rh(H_2tfs)(CO)(PPh_3)).

PPh_3 (7 mg) was aded to a solution of **Rh(H_2tfs)(CO)$_2$** (20 mg) in $CHCl_3$ (30 mL).The mixture was stirred at room temperature for 3 hours, after which the color changed from golden brown to deep-red and TLC (DCM/n-hexane = 1/9) examinations revealed no starting material. Solvent evaporation and chromatography (silica gel, 5-10% DCM in n-hexane) afforded **Rh(H_2tfs)(CO)(PPh_3)** (20 mg, 80% yield). X-ray quality crystals were obtained by recrystallization from DCM and n-heptane. ^{1}H NMR (400 MHz, $CDCl_3$) δ = 12.99 (s, 1H), 9.75 (dd, *J* = 4.7, 2.5, 1H), 9.69 (dq, *J* = 5.4, 2.7, 1H), 9.59 (dd, *J* = 4.7, 2.2, 1H), 9.56 – 9.51 (m, 1H), 9.44 (dd, *J* = 4.4, 2.0, 1H), 9.35 (dd, *J* = 4.9, 2.2, 2H), 9.15 (d, *J* = 4.8, 1H), 6.80 (t, *J* = 7.1, 3H), 6.23 (td, *J* = 8.0, 2.0, 6H), 4.16 (dd, *J* = 11.1, 7.8, 6H), -2.28 (s, 1H), -2.43 (dd, *J* = 4.9, 1.6, 1H), -3.51 (dd, *J* = 4.9, 1.6, 1H). ^{19}F NMR (377 MHz, $CDCl_3$) δ = -36.58 (d, *J* = 53.7, 3F), -39.47 (d, *J* = 72.8, 3F), -45.49 (s, 3F), -47.85 (s, 3F). ^{31}P NMR (162 MHz, $CDCl_3$) δ = 37.81- 36.76 (d, 1P). HRMS$^-$ (APPI, negative mode) for $C_{12}H_{27}ON_5PF_{12}Rh$: m/z = 1039.0811(calculated), 1039.0849 (observed). UV-vis ($CHCl_3$): max (ε(M^{-1} cm^{-1})) = 496 nm (65800), 654 (11000), 703 (12000). IR (neat, cm^{-1}): 1966.

Synthesis of 5, 10, 15-tris(trifluoromethyl)corrolato rhodium(III) (Rh(tfc)(py)$_2$).

A mixture of **H_3(tfc)** (20 mg), dry K_2CO_3 (10 mg), and di-μ-chloro-bis[dicarbonylrhodium(I)] (70 mg) in pyridine (20 mL) was refluxed for 2 h until the disappearance of the starting material (TLC, DCM/n-hexane = 1/9). Solvent evaporation and subsequent silica gel chromatography (DCM/n-hexane/pyridine = 5/95/0.01) afforded **Rh(tfc)(py)$_2$** as a deep-red solid material (19 mg, 82% yield). X-ray quality crystals were obtained by recrystallization from DCM/n-heptane in the presence of two drops of pyridine. ^{1}H NMR (400 MHz, $CDCl_3$) δ = 9.55 (dd, *J* = 5.1, 2.6, 2H), 9.43 (dd, *J* = 5.2, 2.8, 2H), 9.26 – 9.21 (m, 2H), 9.15 (d, *J* = 4.5, 2H), 6.00 (t, *J* = 7.6, 2H), 5.06 (t, *J* = 7.2, 4H), 1.23 (s, 4H). ^{19}F NMR (377 MHz, $CDCl_3$) δ = -36.93 (s, 3F), -39.53 (s, 6F). HRMS$^-$ (ACPI, negative mode) for $C_{22}H_8N_4F_9Rh$: m/z = 601.9655 (calculated), 601.9650 (observed). UV-vis (pyridine): max (ε(M^{-1} cm^{-1})) = 409 nm (90000), 570 (28000).

Acknowledgements

This research was supported by a grant from the Israel Science Foundation. The funding of IS by the Center for Absorption in Science, Ministry of Immigration (KAMEA Foundation), is also acknowledged.

Conflict of interest

The authors declare no conflict of interest.

Keywords: Sapphyrin • Racemization • Porphyrin • Chirality • Cyclopropanation

[1] J. A. Shelnutt, X.-Z. Song, J.-G. Ma, S.-L. Jia, W. Jentzen, C. J. Medforth, *Chem. Sov. Rev.* **1998**, *27*, 31-41.

[2] J. L. Sessler, Z. Gross, H. Furuta, *Chem. Rev.* **2017**, *117*, 2201-2202.

[3] J. L. W. Thudichum, *Rpt. Med. Off. Privy Council* **1867**, *App. 7. 10:152*.

[4] a) R. B. Woodward, *The Chemical Society, London* **1966**, *Special Publication No. 21;* b) V. J. Bauer, D. L. J. Clive, D. Dolphin, J. B. Paine, F. L. Harris, M. M. King, J. Loder, S. W. C. Wang, R. B. Woodward, *J. Am. Chem. Soc.* **1983**, *105*, 6429-6436.

[5] A. W. Johnson, I. T. Kay, *J. Chem. Soc.* **1965**, 1620-1629.

[6] a) Y. S. Balazs, I. Saltsman, A. Mahammed, E. Tkachenko, G. Golubkov, J. Levine, Z. Gross, *Magn. Reson. Chem.* **2004**, *42*, 624-635; b) M. Schlabach, H. H. Limbach, E. Bunnenberg, A. Y. L. Shu, B. R. Tolf, C. Djerassi, *J. Am. Chem. Soc.* **1993**, *115*, 4554-4565; c) J. Braun, M. Schlabach, B. Wehrle, M. Kocher, E. Vogel, H. H. Limbach, *J. Am. Chem. Soc.* **1994**, *116*, 6593-6604; d) K. Rachlewicz, N. Sprutta, L. Latos-Grażyński, P. J. Chmielewski, L. Szterenberg, *J. Chem. Soc., Perkin Trans. 2* **1998**, 959-967; e) P. J. Chmielewski, L. Latos-Grażyński, K. Rachlewicz, *Chem. Eur. J* **1995**, *1*, 68-73.

[7] A. E. Meier-Callahan, H. B. Gray, Z. Gross, *Inorg. Chem.* **2000**, *39*, 3605-3607.

[8] J. F. Barata, M. G. Neves, M. A. Faustino, A. C. Tome, J. A. Cavaleiro, *Chem. Rev.* **2017**, *117*, 3192-3253.

[9] a) R. D. Teo, J. Y. Hwang, J. Termini, Z. Gross, H. B. Gray, *Chem. Rev.* **2017**, *117*, 2711-2729; b) W. Zhang, W. Lai, R. Cao, *Chem. Rev.* **2017**, *117*, 3717-3797; c) Z. Gross, N. Galili, I. Saltsman, *Angew. Chem. Int. Ed.* **1999**, *38*, 1427-1429.

[10] a) W. Shan, N. Desbois, V. Blondeau-Patissier, M. L. Naitana, V. Quesneau, Y. Rousselin, C. P. Gros, Z. Ou, K. M. Kadish, *Chem. Eur. J.* **2017**, *23*, 12833-12844; b) T. Chatterjee, A. Srinivasan, M. Ravikanth, T. K. Chandrashekar, *Chem. Rev.* **2017**, *117*, 3329-3376.

[11] D. Mori, T. Yoneda, T. Hoshino, S. Neya, *Chem. Asian. J.* **2018**, *13*, 934-938;

[12] L. Simkhovich, S. Rosenberg, Z. Gross, *Tetrahedron Lett.* **2001**, *42*, 4929-4931.

[13] A. Jasat, D. Dolphin, *Chem. Rev.* **1997**, *97*, 2267-2340.

[14] W. Huang, Z. Ou, X. Chen, Z. Xue, G. Lu, H. Wang, J. Xiao, Y. Fang, K. M. Kadish, *J. Porphyrins Phthalocyanines* **2015**, *19*, 794-802.

[15] A. K. Burrell, J. L. Sessler, M. J. Cyr, E. McGhee, J. A. Ibers, *Angew. Chem. Int. Ed.* **1991**, *30*, 91-93.

[16] Q. C. Chen, M. Soll, A. Mizrahi, I. Saltsman, N. Fridman, M. Saphier, Z. Gross, *Angew. Chem. Int. Ed.* **2018**, *57*, 1006-1010.

[17] a) S. J. Narayanan, B. Sridevi, T. K. Chandrashekar, U. Englich, K. Ruhlandt-Senge, *Inorganic Chemistry* **2001**, *40*, 1637-1645. b) J. L. Sessler, A. H. Burrell, J. Lisowski, A. Gebauer, M. J. Cyr, V. Lynch, *Bull. Soc. Chem. Fr.* **1996**, *133*, 725-743.

[18] I. Saltsman, L. Simkhovich, Y. Balazs, I. Goldberg, Z. Gross, *Inorganica Chim. Acta* **2004**, *357*, 3038-3046.

[19] J. H. Palmer, A. Mahammed, K. M. Lancaster, Z. Gross, H. B. Gray, *Inorg. Chem.* **2009**, *48*, 9308-9315.

[20] a) Y. Chen, K. B. Fields, X. P. Zhang, *J. Am. Chem. Soc.* **2004**, *126*, 14718-14719; b) C. M. Che, J. S. Huang, F. W. Lee, Y. Li, T. S. Lai, H. L. Kwong, P. F. Teng, W. S. Lee, W. C. Lo, S.mM. Peng, Z. Y. Zhou, *J. Am. Chem. Soc.* **2001**, *123*, 4119-4129.

[21] D. W. Bartley, T. Kodadek, *J. Am. Chem. Soc.* **1993**, *115*, 1656-1660.

[22] a) H. J. Callot, C. Piechocki, *Tetrahedron Lett.* **1980**, *21*, 3489-3492; b) S. J. Thompson, M. R. Brennan, S. Y. Lee, G. Dong, *Chem. Soc. Rev.* **2018**, *47*, 929-981.

[23] a) T. Tanaka, A. Osuka, *Chem. Rev.* **2017**, *117*, 2584-2640; b) B. Szyszko, M. J. Bialek, E. Pacholska-Dudziak, L. Latos-Grazynski, *Chem. Rev.* **2017**, *117*, 2839-2909.

[24] Z. S. Yoon, S. B. Noh, D. G. Cho, J. L. Sessler, D. Kim, *Chem. Commun.* **2007**, 2378-2380.

[25] G. W. T. M. J. Frisch, H. B. Schlegel, G. E. Scuseria, M. A. Robb, J. R. Cheeseman, G. Scalmani, V. Barone, B. Mennucci, G. A. Petersson, H. Nakatsuji, M. Caricato, X. Li, H. P. Hratchian, A. F. Izmaylov, J. Bloino, G. Zheng, J. L. Sonnenberg, M. Hada, M. Ehara, K. Toyota, R. Fukuda, J. Hasegawa, M. Ishida, T. Nakajima, Y. Honda, O. Kitao, H. Nakai, T. Vreven, J. A. Montgomery Jr., J. E. Peralta, F. Ogliaro, M. J. Bearpark, J. Heyd, E. N. Brothers, K. N. Kudin, V. N. Staroverov, R. Kobayashi, J. Normand, K. Raghavachari, A. P. Rendell, J. C. Burant, S. S. Iyengar, J. Tomasi, M. Cossi, N. Rega, N. J. Millam, M. Klene, J. E. Knox, J. B. Cross, V. Bakken, C. Adamo, J. Jaramillo, R. Gomperts, R. E. Stratmann, O. Yazyev, A. J. Austin, R. Cammi, C. Pomelli, J. W. Ochterski, R. L. Martin, K. Morokuma, V. G. Zakrzewski, G. A. Voth, P. Salvador, J. J. Dannenberg, S. Dapprich, A. D. Daniels, Ö. Farkas, J. B. Foresman, J. V. Ortiz, J. Cioslowski, D. J. Fox, Gaussian, Inc., Wallingford, CT, USA, 2009.

[26] a) C. Adamo, V. Barone, *J. Chem. Phys.* **1999**, 110, 6158-6170; b) S. Grimme, J. Antony, S. Ehrlich, H. Krieg, *J. Chem. Phys.* **2010**, 132, 154104-154123.

[27] A. V. Marenich, C. J. Cramer, D. G. Truhlar, *J. Phys. Chem. B* **2009**, *113*, 6378-6396.

[28] a) U. Häussermann, M. Dolg, H. Stoll, H. Preuss, P. Schwerdtfeger, R. M. Pitzer, *Mol. Phys.* **1993**, *78*, 1211-1224; b) W. Küchle, M. Dolg, H. Stoll, H. Preuss, *J. Phys. Chem.* **1994**, *100*, 7535-7542; c) T. Hangele, M. Dolg, M. Hanrath, X. Cao, P. Schwerdtfeger, *J. Chem. Phys.* **2012**, *136*, 214105.

[29] a) K. Fukui, *Acc. Chem. Res.* **1981**, *14*, 363-368; b) K. Fukui, *J. Phys. Chem.* **1970**, *74*, 4161-4163.

[30] M. A. Spackman, D. Jayatilaka, *CrystEngComm* **2009**, *11*, 19-32.

[31] S. K. Wolff, D. J. Grimwood, J. McKinnon, M. J. Turner, D. Jayatilaka, M. A. Spackman, *CrystalExplorer (Version 3.1)* **2012**, *University of Western Australia*.

[32] D. Kappa CCD Server Software; Nonius BV, The Netherlands, **1997**.

[33] Z. Otwinowski, W. Minor, *Methods Enzymol.* **1997**, *276*, 307-326.

[34] G. M. Sheldrick, *Acta Crystallogr. A* **1990**, *46*, 467-473.

[35] L. Simkhovich, A. Mahammed, I. Goldberg, Z. Gross, *Chem. Eur. J.* **2001**, *7*, 1041-1055.

10.1002/chem.201804138

WILEY-VCH

Entry for the Table of Contents (Please choose one layout)

Layout 1:

FULL PAPER

Text for Table of Contents

Larger affinity to rhodium, easy resolution of racemic rhodium(I) complexes, and increased selectivity to the kinetic cyclypropanation product are some of the unique features displayed by the *meso*-CF_3-subsituted sapphyrin.

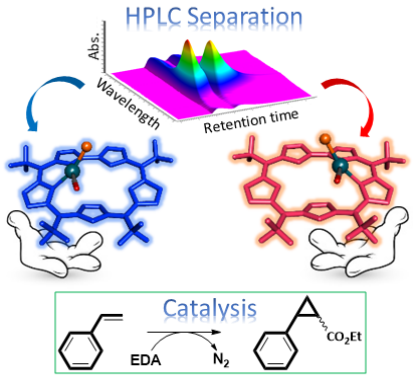

*Author(s), Corresponding Author(s)**

Page No. – Page No.

Title

Layout 2:

FULL PAPER

((Insert TOC Graphic here; max. width: 11.5 cm; max. height: 2.5 cm))

*Author(s), Corresponding Author(s)**

Page No. – Page No.

Title

Text for Table of Contents